EPC method for delamination assessment of basalt FRP pipe: electrodes number effect

Wael A. Altabey[*1,2]

[1]*International Institute for Urban Systems Engineering, Southeast University, Nanjing (210096), China*
[2]*Department of Mechanical Engineering, Faculty of Engineering,*
Alexandria University, Alexandria (21544), Egypt

Abstract. Delamination is the most common failure mode in layered composite materials. The author have found that the electrical potential change (EPC) technique using response surfaces method is very effective in assessment delamination in basalt fiber reinforced polymer (FRP) laminate composite pipe by using electrical capacitance sensor (ECS). In the present study, the effect of the electrodes number on the method is investigated using FEM analyses for delamination location/size detection by ANSYS and MATLAB, which are combined to simulate sensor characteristic. Three cases of electrodes number are analyzed here are eight, twelve and sixteen electrodes, afterwards, the delamination is introduced into between the three layers [0º/90º/0º]s laminates pipe, split into eight, twelve and sixteen scenarios for cases of eight, twelve and sixteen electrodes respectively. Response surfaces are adopted as a tool for solving inverse problems to estimate delamination location/size from the measured EPC of all segments between electrodes. As a result, it was revealed that the estimation performances of delamination location/size depends on the electrodes number. For ECS, the high number of electrodes is required to obtain high estimation performances of delamination location/size. The illustrated results are in excellent agreement with solutions available in the literature, thus validating the accuracy and reliability of the proposed technique.

1. Introduction

Delamination is the most common damage in composite materials during manufacturing and subsequent operational effects such as impact loads, fatigue, etc. Since a delamination in a laminated composite is usually hidden between layers, it is very difficult to detect the delamination while the composite structure is in service, thus causing low reliability. To ensure the integrity and reliability operating composite components, an expert system for delamination monitoring for applications that the composite structures under service is required.

Non-destructive testing (NDT) methods have been found to be useful for in-situ evaluation of composites structures, where the structural integrity of laminate composite structures can be

---

∗Corresponding author, Assistant Professor, E-mail: wael.altabey@gmail.com

assessed effectively. Recently, various methods have been implemented for laminate composite structures monitoring including Ultrasonic (Amaro *et al.* 2011, Zeng Hua *et al.* 2013, Liu *et al.* 2014); X-Ray Radiography (De Albuquerque *et al.* 2010, Tompson and Johnson 2011); Thermography (Toscano *et al.* 2012); Acoustic Emission (Davijani *et al.* 2011, Saeedifar *et al.* 2015, Saeedifar *et al.* 2016); Vibrography (Garcia *et al.* 2015, Cunedioglu and Beylergil 2015); Eddy Currents (Heuer *et al.* 2013); Optical-based nondestructive techniques including embedded Optical Fiber Sensors (Peng *et al.* 2012), and Lamb Wave (Hu *et al.* 2010, Yeum *et al.* 2012, Nguyen *et al.* 2013, Spiegel 2014).

As we see, there is a diverse range of NDE techniques for detecting delamination in composite structures, and the capabilities and limitations of each method are different. Each technique has its specific field of applicability although there is a level of overlap according to delamination identification and accuracy of detection and the ability to detect delamination location/size. For example, it may be necessary to combine information gained from ultrasonics and X-ray radiography to achieve a three-dimensional map of the complex array of delamination location/size in a composite, but no single method is capable of detecting all delamination identification with high accuracy, easy and low-cost.

ECS is one of the most mature and promising NDE methods, which measures the capacitance change of multi-electrode sensor due to the change of dielectric permittivity. It has the characteristics such as low cost, fast response, non-intrusive method, broad application, safety (Yang *et al.* 1995a, 1995b, Li and Huang 2000, Mohamad *et al.* 2012, Zhang *et al.* 2014). The need for a more accurate measurement of ECS led to the study of the factors which have influence and effect on ECS sensitivity and sensitive domain of ECS electrodes. There are three factors have been studied and found which have effect on ECS measurements, i.e., pipeline material, inner dielectric permittivity (Jaworski and Bolton 2000, Pei and Wang 2009, Al-Tabey 2010, Asencio *et al.* 2015, Sardeshpande *et al.* 2015, Mohamad *et al.* 2016, Altabey 2016) and the ratio of pipeline thickness and diameter (Daoye *et al.* 2009, Altabey 2016), later Altabey (2016) found that the ECS environment temperature has effect on ECS sensitivity and sensitive domain of ECS electrodes with high percentage, so the environment temperature is the fourth factor of factors which have influence on ECS measurement sensitivity.

To improve the estimation performance of the delamination location/size with the electrical potential change (EPC) technique, this work proposed new method with normalizations of the EPC method data and studied the effect of the ECS electrodes number on estimation performance of the delamination using FE analyses by ANSYS and MATLAB software. The measured electric potential differences between electrodes were normalized, and the response surfaces to estimate the delamination location/size were made from the normalized electric potential differences and the norm. The new method has been applied to estimate the delamination location/size in basalt FRP laminate composite pipe and the estimation performance is found to be significantly improved. The estimation performances of each case of electrodes number are compared with each other, and the width of the error band of the estimations of delamination length is obtained and the estimation performance was found to be significantly improved.

2. Principle of Electrical Capacitance sensor (ECS)

ECS was first introduced in the 1980s by a group of researchers from the US Department of Energy Morgantown Energy Technology Center (METC), to measure fluidized bed system
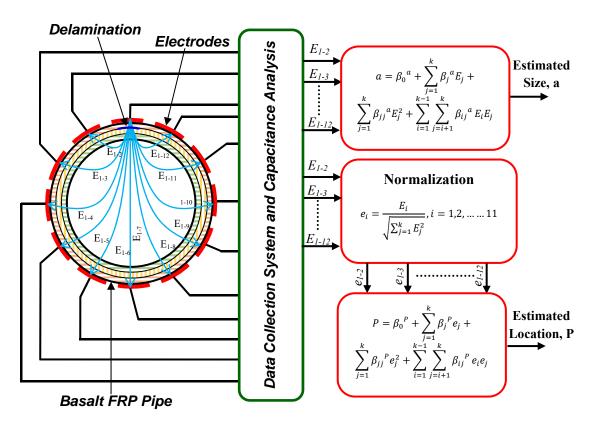
Fig. 1 Sketch of 12-electrode ECS system with response surfaces method

(Fasching and Smith 1988, Fasching and Smith 1991, Huang *et al.* 1989). The technique has been developed rapidly during the past 10 years, and then they have become popular and gained importance to monitor industrial processes due to its low cost and its operability under harsh environmental conditions.

ECS consists of insulating pipe, measurement electrode, radial screen and earthed screen (Yang and York 1999). The measurement electrode is mounted symmetrically around the circumference of pipeline. Radial screen is fitted between the electrodes to cut the electro-line external to the sensor pipeline and reduce the inter-electrode capacitance. The earthed screen surrounds the measurement electrodes to shield external electromagnetic noise. In most application, ECS electrode is mounted outside the pipeline which is called external electrode ECS (Yang 1997). Electrical capacitance system includes sensor, capacitance measuring circuit when electrode (1) is excited with response surfaces method is shown in Fig. 1.

2.1 The ECS composition and working principle

For 12-electrode system, the electrodes are numbered as shown in the Fig. 2, the electrodes are excited with an electric potential, one at the time in increasing order, when one electrode is excited, the other electrodes are kept at ground potential and act as detector electrodes as shown in the Fig. 2. When electrode No. 1 is excited with a potential, the change $Q_{1,j}$ is induced on the
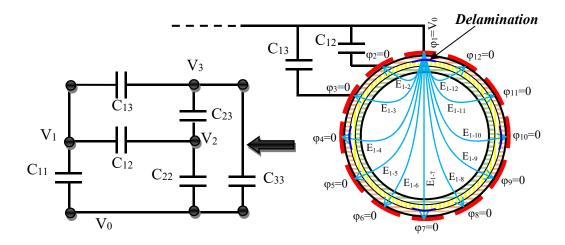
Fig. 2 Schematic representation of the measurement principle of an ECS for case of 12-electrode

electrodes, $j = 2, \cdots\cdots, N$ can be measured. Next, electrode No. 2 is excited whereas, rest the electrodes are kept at ground potential, and the induced charges $Q_{23}, Q_{24}, \cdots, Q_{2N}$ ($N = 8, 12, 16$) are measured. The measurement protocol continues unit electrode $N - 1$ is excited. Using these charge measurements, the inter electrode capacitance C_{ij} can be computer using the definition of capacitance (Eq. (1)) i.e.

$$C_{ij} = \frac{Q_{ij}}{\Delta V_{ij}} \tag{1}$$

Where Q_{ij} is the charge induced on electrode j when electrode i is excited with a known potential. V_{ij} is the potential difference between electrodes i and j $\left(\Delta V_{ij} = V_i - V_j\right)$. So the number of independent capacitance measurements $M = 28, 66, 120$ for $N = 8, 12, 16$ respectively using Eq. (2) is

$$M = \frac{N(N-1)}{2} \tag{2}$$

3. Finite element simulation model

3.1 ECS System geometrical model

Fig. 3 shows the cross section of 12electrode ECS system. The sensors physical specifications and the permittivity values of basalt FRP composite pipe are shown in Table 1.

3.2 Physical properties of the basalt FRP pipe

Physical and mechanical properties of the basalt FRP laminate composite pipe are shown in Table 2.

Table 1 Sensor physical specification

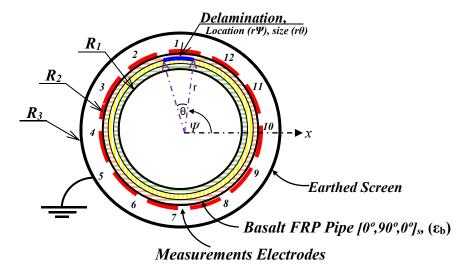| ECS system	Specification
No. of electrodes	8, 12, 16
Space between electrodes	3, 2, 1 mm
Pipe diameter (d_i)	94 mm
Pipe thickness (h)	6 mm
Earth Screen diameter	110 mm
Thickness of electrodes	1mm
height of electrodes	0.3 m
Permittivity Basalt fiber/Polymer	$\varepsilon_b = 2.2$ Fm^{-1}
Permittivity of Water	$\varepsilon_w = 80$ Fm^{-1}
Permittivity of Air	$\varepsilon_a = 1.0$ Fm^{-1}
Excitation voltage	$\varphi = 15$ Volts

Fig. 3 Cross section sketch of 12-electrode ECS

Table 2 Physical and mechanical properties of the basalt FRP

E_1	$E_2 = E_3$	$G_1 = G_3$	G_2	$v_1 = v_3$	v_2	ρ
96.74GPa	22.55GPa	10.64GPa	8.73GPa	0.3	0.6	2700 kg/m^3

3.3 ECS Governing equation

In terms of Electrical Capacitance sensor (ECS), the forward problem is the problem of calculating the capacitance matrix C from a given set of sensor design parameters and a given cross-sectional permittivity distribution $\varepsilon(x, y)$

$$\nabla . \varepsilon(x, y) \nabla \varphi(x, y) = 0 \tag{3}$$

Where: $\varphi(x,y)$ is the potential distribution inside the ECS is determined by solving the Poisson's equation. For the boundary condition imposed on the ECS head by the measurement system. The electric field vector $E(x,y)$, the electric flux density $D(x,y)$ and the potential function $\varphi(x,y)$ are related as follows

$$E(x,y) = -\nabla\varphi(x,y) \qquad (4)$$

$$D = \varepsilon(x,y)E(x,y) \qquad (5)$$

The change on the electrodes, and hence the inter electrode capacitances can be found using the definition of the capacitance and Gauss's law based on the following surface integral

$$Q_{ij} = \oint_{S_j} (\varepsilon(x,y)\nabla\varphi(x,y).\hat{n})\,ds \qquad (6)$$

Where: $\nabla.\varepsilon(x,y)$ is the divergence of permittivity distribution, $\nabla\varphi(x,y)$ is the gradient of potential distribution, S_j is a surface enclosing electrode j, ds is an infinitesimal area on electrode j, $\hat{n}$ is the unit vector normal to S_j and ds is an infinitesimal area on that.

3.4 The FE model description

In this section, the numerical models for simulating the delamination scenarios in basalt FRP pipe will be addressed using ANSYS ver.15. 2D FE software. The approach taken by ANSYS 2D is to divide the different materials and geometries into triangular elements, because many pipes are round under the circumstances of a smaller number of pixels, we can achieve higher accuracy to use the triangular mesh instead of rectangular grids, and then to represent the electric field (see Eq. (4)) within each element with a separate polynomial at six integration points location. For FE simulating of basalt FRP pipe, electrostatic module (PLANE121), triangular 6-node, and the element has one degree of freedom, voltage, at each node. The 6-node elements have compatible voltage shapes and are well suited to model curved boundaries. The total number of elements used for the analyses was 4873. To improve the accuracy of mesh, we divided the meshed region again into 9798 elements.

The potential boundary conditions were applied to the sensor-plate (electrodes). For one electrode, the boundary condition of electric potential (V=V_0) with 15V (V_0) was applied and another electrode was kept at ground (V=0) potential to simulate a 15V (RMS) potential gradient across the electrodes. For representing the natural propagation of electric field, the default boundary condition of continuity ($\hat{n}.(D_1 - D_2) = 0$) was maintained for the internal boundaries.

4. Response surface for the electric potential differences method

The response surface is a widely adopted tool for quality engineering fields (Myers and Montgomery 2002). The response surface methodology brings two advantages, the inverse problems can be approximately solved without consideration of modeling, and the approximated response surfaces can be evaluated using powerful statistical tools. In the present study, the response surface methodology was adopted as a solver for predicting of the delamination locations/sizes from measured electric potential difference, this is one of the inverse problems (see Fig. 1). For most of the response surfaces, the functions for the approximations are polynomials

because of simplicity. For the cases of quadratic polynomials, the response surface is described as follow

$$y = \beta_0 + \sum_{j=1}^{k} \beta_j x_j + \sum_{j=1}^{k} \beta_{jj} x_j^2 + \sum_{i=1}^{k-1} \sum_{j=i+1}^{k} \beta_{ij} \, x_i x_j \tag{7}$$

Where k is the number of variables, k is depend on the electrodes number. In this study the number of variables are 8, 12 and 16 electric potential difference variable; for 8, 12 and 16 electrode respectively, e.g., in the case of the 12-electrode, there are 12 electric potential differences variables; V_0, E_{1-2}, E_{1-3},…... and E_{1-12}, y is the response surface for estimations of delamination location (Ψ) and size (θ) and the coefficients β are obtained with the least square errors method (Myers and Montgomery 2002, Jiang *et al.* 2014).

To improve the estimation performance of the delamination location/size, the normalizations of the measured electric potential differences are performed. Each element is divided by the square root sum and replacement the vector (E_{1-2}, E_{1-3},..., E_{1-12}) in Eq. (7) with norm vector (e_{1-2}, e_{1-3},…, e_{1-12}) as shown in Fig. 1.

In the case that varies delamination scenarios, the total number of scenarios is n, the response surface can be expressed as follows using matrix expression

$$Y = X\beta + \lambda \tag{8}$$

Where: $Y = \begin{Bmatrix} y_1 \\ y_2 \\ \vdots \\ y_n \end{Bmatrix}$, $X = \begin{bmatrix} 1 & x_{11} & x_{12} & \dots & x_{1k} \\ 1 & x_{21} & x_{22} & \dots & x_{2k} \\ \vdots & \vdots & \vdots & \ddots & \vdots \\ 1 & x_{n1} & x_{n2} & \dots & x_{nk} \end{bmatrix}$, $\beta = \begin{Bmatrix} \beta_0 \\ \beta_1 \\ \vdots \\ \beta_k \end{Bmatrix}$, $\lambda = \begin{Bmatrix} \lambda_1 \\ \lambda_2 \\ \vdots \\ \lambda_n \end{Bmatrix}$

Where λ is an error vector. The unbiased estimator b of the coefficient vector β is obtained using the well-known least square error method as follows

$$b = (X^T X)^{-1} + X^T Y \tag{9}$$

The variance-covariance matrix of the b is obtained as follows

$$Cov(b_i, b_j) = \sigma^2 \, (X^T X)^{-1} \tag{10}$$

Where the σ is the error of Y. The estimated value of σ is obtained as follows

$$\sigma^2 = \frac{SS_E}{n-k-1} \tag{11}$$

SS_E is a square sum of errors, and expressed as follows

$$SS_E = Y^T Y - b^T \, X^T Y \tag{12}$$

The lack of fit is evaluated with the adjusted coefficient of the multiple determination $R^2_{\,adj}$ (Myers and Montgomery 2002); $R^2_{\,adj}$ is defined as

$$R^2_{\,adj} = 1 - \frac{SS_E/(n-k-1)}{S_{yy}/(n-1)} \tag{13}$$

Where S_{yy} is the total sum of squares

$$S_{yy} = Y^T Y - \frac{\left(\sum_{i=1}^{n} y_i\right)^2}{n} \tag{14}$$

The value of $R^2_{\,adj}$ is equal to or lower than 1.0. A higher value of $R^2_{\,adj}$ implies a better fit. When the response surface shows a very good fit, $R^2_{\,adj}$ approaches 1.0. A good fit of the

response surface means that the response surface gives good estimations for the electrical potential (EP) technique used for the regression. Lower $R^2{}_{adj}$ values means poorer estimations and the error band of the estimated result is wider.

5. Results and discussion

5.1 Convergence study and accuracy

In this subsection, a convergence investigation is carried out for the proposed method. The normalization electrical potential differences between electrodes due to delamination are calculated and compared with available experimental results in literatures. The dataset used for validation of presented technique is adapted from (Todoroki *et al.* 2004). The tests were conducted on composite laminated beams were manufactured from unidirectional layers of carbon/epoxy (CFRE). The stacking sequence is $[0_2/90_2]_s$ and the thickness of the laminates is approximately t=1 mm. The fiber volume fraction is approximately V_f=0.5. The beam type specimens have the length of 270 mm and the width of 15 mm. Seven electrodes are mounted on the specimen surface. All of these electrodes are placed on a single side of a specimen. For electrode model, the thickness of electrodes is 10 mm, the space between electrodes is 45 mm and the boundary condition of electric potential (V=V_0) with +5V (V_0). The electrical potential changes of each segment between electrodes are measured for various cases of location and size of delaminations. From the

Table 3 Convergence study of normalization electrical potential differences of the CFRE laminated composite beams

e_{1-2}	(1)	0.9918	0.2922	0.6931	0	0	0.6315	0.1897	0.0105	0.3158	0.0184
	(2)	0.9914	0.2873	0.6877	0	-0.0057	0.6007	0.1869	0.0059	0.3111	0.0139
e_{2-3}	(1)	0.0015	0.3512	0.7177	0.1683	0	0.3724	0.3711	0.0158	0.4531	0.0187
	(2)	-0.1305	0.3478	0.7127	0.1669	-0.0172	0.3682	0.3686	0.0094	0.4470	0.0139
e_{3-4}	(1)	0	0.4497	0.1380	0.5911	0.5125	0.5848	0.7355	0.0008	0.3992	0
	(2)	0	0.4461	0.1375	0.5881	0.5113	0.5813	0.7294	0	0.3976	0
e_{4-5}	(1)	0	0.5243	0.0173	0.6786	0.7826	0.4106	0.5473	0	0.5481	0.2392
	(2)	0	0.5217	0.0125	0.6754	0.7814	0.4069	0.5451	0	0.5457	0.2371
e_{5-6}	(1)	0	0.3269	0	0.3721	0.2894	0.0006	0	0.5900	0.4711	0.2671
	(2)	0	0.3251	-0.0125	0.3698	0.2873	0	0	0.5885	0.4692	0.2650
e_{6-7}	(1)	0	0.4699	0	0.1856	0.2175	0	0	0.8111	0.1683	0.9369
	(2)	0	0.4687	0	0.1823	0.2126	0.0065	-0.0026	0.8085	0.1655	0.9344
Location	(1)	-127.35	-113.23	-81.53	-68.37	-18.22	7.86	19.58	67.34	97.39	108.19
	(2)	-127.5	-113.5	-82	-69	-18.5	8	20	68	98	109
Size	(1)	5.48	4.87	1.96	5.46	5.92	2.91	5.96	8.48	5.98	4.95
	(2)	5.5	5	2	5.5	6	3	6	8.5	6	5

[1] Proposed method, [2] Todoroki *et al.* (2004)

measured data, the relationships between electrical potential change and location and the size of the delaminations are obtained using response surface method. Table 3 presents a convergence and comparison study for the proposed method data and the experimental data of (Todoroki *et al.* 2004).

From Table 3 it can be observed that the numerical results are in an excellent agreement with experimental results of normalization electrical potential differences presented by (Todoroki *et al.* 2004). This validates the precision of the presented technique.

5.2 Electrical potential (EP) technique for delamination assessing

To investigate the effect of the delamination on the dielectric properties in basalt FRP pipe, the FE analysis of the electric field intensity of basalt FRP piping system were performed using commercially available FE code ANSYS (The Electrostatic Module in the Electromagnetic subsection of ANSYS (2015), Al-Tabey 2012). The software only computes the potential and the electric field values at the element nodes and interpolate between these nodes to obtain the values for other points within the elements.

To study the effect of the electrodes number on the ECS results, the three cases of the electrodes number analyzed here are 8, 12 and 16 electrodes, at each case of electrodes number, the various of delamination scenarios of delamination location/size are used for validating the accuracy and reliability of the proposed technique. In order to give good accuracy and reliability in each case of electrodes number, the number of delamination scenarios in each case are different and depend on

Table 4 FE results of electric potential differences for each case of electrodes number

$Del_{(\Psi,0)}$	E_{1-1}	E_{1-2}	E_{1-3}	E_{1-4}	E_{1-5}	E_{1-6}	E_{1-7}	E_{1-8}	E_{1-9}	E_{1-10}	E_{1-11}	E_{1-12}	E_{1-13}	E_{1-14}	E_{1-15}	E_{1-16}
						Electric potential differences (V)										
							8-Electrodes									
Del_0	15	7.28	3.92	3.33	3.1	3.33	3.92	7.28	---	---	---	---	---	---	---	---
$Del_{(0,5)}$	15	7.28	3.92	3.33	3.1	3.33	**3.25**	7.28	---	---	---	---	---	---	---	---
$Del_{(90,10)}$	15	**6.97**	**3.65**	**3.14**	**2.9**	**3.14**	**3.65**	**6.97**	---	---	---	---	---	---	---	---
$Del_{(180,15)}$	15	7.28	**3.25**	3.33	3.1	3.33	3.92	7.28	---	---	---	---	---	---	---	---
$Del_{(270,20)}$	15	7.28	3.92	3.33	**2.89**	3.33	3.92	7.28	---	---	---	---	---	---	---	---
							12-Electrodes									
Del_0	15	7.5	4.93	4.03	3.7	3.57	3.57	3.57	3.7	4.03	4.93	7.5	---	---	---	---
$Del_{(0,5)}$	15	7.5	4.93	4.03	3.7	3.57	3.57	3.57	3.7	**3.33**	4.93	7.5	---	---	---	---
$Del_{(90,10)}$	15	**7.2**	**4.3**	**3.82**	**3.53**	**3.33**	**2.5**	**3.33**	**3.53**	**3.82**	**4.3**	**7.2**	---	---	---	---
$Del_{(180,15)}$	15	7.5	4.93	**3.33**	3.7	3.57	3.57	3.57	3.7	4.03	4.93	7.5	---	---	---	---
$Del_{(270,20)}$	15	7.5	4.93	4.03	3.7	3.57	**3**	3.57	3.7	4.03	4.93	7.5	---	---	---	---
							16-Electrodes									
Del_0	15	7.87	5.45	4.86	4.55	4.29	3.93	3.61	3.61	3.61	3.93	4.29	4.55	4.86	5.45	7.87
$Del_{(0,5)}$	15	7.87	5.45	4.86	4.55	4.29	3.93	3.61	3.61	3.61	3.93	4.29	**4.35**	4.86	5.45	7.87
$Del_{(90,10)}$	15	**7.58**	**5.26**	**4.62**	**4.39**	**3.1**	**3.72**	**3.52**	**3.52**	**3.52**	**3.72**	**3.1**	**4.39**	**4.62**	**5.26**	**7.58**
$Del_{(180,15)}$	15	7.87	5.45	4.86	**4.35**	4.29	3.93	3.61	3.61	3.61	3.93	4.29	4.55	4.86	5.45	7.87
$Del_{(270,20)}$	15	7.87	5.45	4.86	4.55	4.29	3.93	3.61	**3.42**	3.61	3.93	4.29	4.55	4.86	5.45	7.87

the electrodes number that mounted around the outer surface of the basalt FRP pipe, in general this study must be used at least 8, 12 and 16 delamination scenarios for 8, 12 and 16 electrodes respectively, i.e., the same number of electrodes according to each case of electrodes number.

To study the behavior of ECS working under varying of the delamination location/size data for each case of electrodes number, we are selected four various scenarios of the delamination location/size in basalt FRP laminate composite pipe are applied for each electrode number, the first scenario ($Del_{(0,5)}$) has size $\theta=5°$, is located at $r=51$ mm and $\Psi=0°$, the second scenario ($Del_{(90,10)}$) has size $\theta=10°$, is located at $r=51$ mm and $\Psi=90°$, the third delamination scenario ($Del_{(180,15)}$) has size $\theta=15°$, is located at $r=51$ mm and $\Psi=180°$ and final scenario ($Del_{(270,20)}$) has size $\theta=20°$, is located at $r=51$ mm and $\Psi=270°$, respectively, as shown in Table 4 of FE results of electric potential differences before (Del_0) and after ($Del_{(\Psi,\theta)}$) delamination for each case of electrodes number, where Ψ is the angle of delamination location and θ is the angle of delamination size in degree (see Fig. 3).

Using the scripting capabilities in ANSYS we can be simulated capacitance values (C_{ij}) and potential differences (E_{ij}) between electrodes, before (Del_0) and after ($Del_{(\Psi,\theta)}$) introduced delamination.

As shown in the Table 4 of the electrical potential differences (E_{i-j}) with different scenarios of delamination location/size and each case of electrodes number when electrode (1) is excited, we can see the effect of the delamination on the electrical potential distributions, this degradation is occurred only in the values of the potential differences according to the electrode that mounted close to the location of delamination occurred. For example, as shown in Fig. 4 of plot for electrical potential distributions in Table 4 for case of 12- electrode ECS system, the degradation in E_{1-4} is due to delamination scenario ($Del_{(180,15)}$), E_{1-7} is due to scenario ($Del_{(270,20)}$) and E_{1-10} is due to scenario ($Del_{(0,5)}$). Except delamination scenario ($Del_{(90,10)}$) is influenced on the all potential differences from E_{1-2} to E_{1-12}, because, delamination is located close to the excited electrode (1), and so on this behavior will be repeated when the other electrode is excite, (see Fig. 2), this
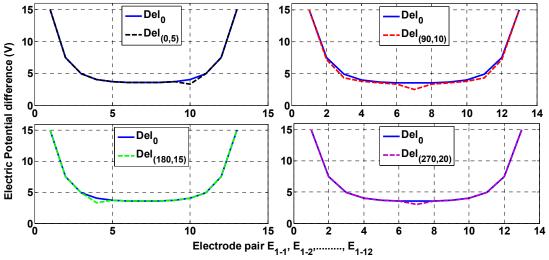

Fig. 4 Effect of delamination scenarios ($Del_{(\Psi,\theta)}$)on electric potential difference (V) when electrode (1) is excited for the case of 12- electrode ECS system

conclusion also found for other cases of electrodes number but with difference electrode pair, i.e., the degradation is appeared in different potential differences (see Table 4) (e.g., delamination scenario ($Del_{(0,5)}$) is causes degradation in E_{1-7} for 8-electrodes ECS, but it causes degradation in E_{1-13} for 16-electrodes ECS, etc.).

The 66 capacitance measurements (C_{ij}) for each delamination scenarios in basalt FRP composite pipe for case of 12- electrode ECS system are illustrated together in Fig. 5. As shown in the Fig. 5, we can see that the effect of the delamination occurred on the capacitance measurements (C_{ij}) distributions the degradation in capacitance values between electrodes is occurred, this degradation depends on the delamination size (θ), as increases of the delamination size (θ), the capacitance values decreased.

Fig. 6 show the sensor sensitivity with versus delamination scenarios ($Del_{(\Psi,\theta)}$) for electrode number is 8, 12 and 16 respectively. The sensor sensitivity is defined as

$$Sensor\ sensitivity\% = \frac{C_{ij(del_0)} - C_{ij(del_{(\Psi,\theta)})}}{C_{ij(del_0)}} \times 100 \qquad (15)$$

Where $C_{ij(del_0)}$ and $C_{ij(del_{(\Psi,\theta)})}$ are the capacitance measurements between electrode pairs (i-j) before and after delamination occurred respectively for each scenario of the delamination location (Ψ) and size (θ).

As shown in the Fig. 6, for each case of the electrodes number, the sensor sensitivity for delamination monitoring depends on the delamination size (θ) and the electrodes number are mounted on the outer surface of the basalt FRP pipe, as the electrodes number or delamination size (θ) increased, the sensor sensitivity is increased.
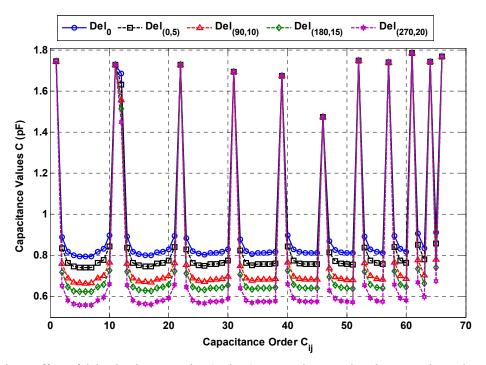

Fig. 5 Effect of delamination scenarios ($Del_{(\Psi,\theta)}$)on capacitance values between electrodes
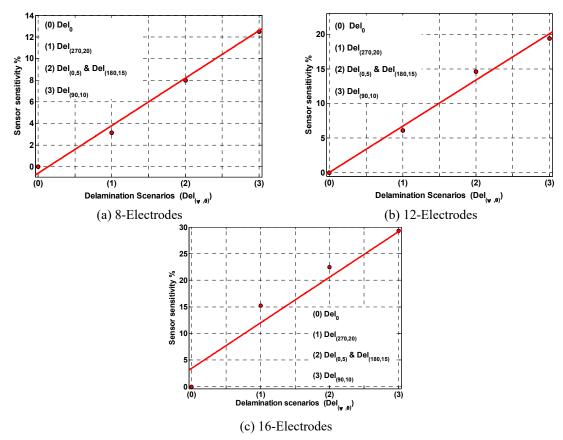
(a) 8-Electrodes

(b) 12-Electrodes

(c) 16-Electrodes

Fig. 6 Capacitance sensor sensitivity versus delamination scenarios (Del$_{(\Psi, \theta)}$)

The sensor has a sensitivity ranging between (3.15 and 12.53%), (6.13 and 19.369%) and (15.24 and 29.32%) for 8-electrodes, 12-electrodes and 16-electrodes respectively and selected sensor geometrical parameters.

5.3 Estimation of delamination location/size

Figs. 7 and 8 show a comparison between the estimated results of the delamination location, Ψ and size, θ for each cases of electrodes number in basalt FRP laminate composite pipe by using response surface method.

The R^2_{adj} of estimated location are 0.8922, 0.9625 and 0.9943 for 8-electrode, 12-electrode and 16-electrode respectively and estimated size are 0.8428, 0.9357 and 0.9897 for 8-electrode, 12-electrode and 16-electrode respectively. All of the estimations are plotted on the diagonal line. The error band is defined as the maximum error of the estimated location and size. The error band from the diagonal line of estimated location is less than 11.3, 8 and 3.4 degrees for 8-electrode, 12-electrode and 16-electrode respectively and estimated size is less than 5.6, 2.5 and 1 degrees for 8-electrode, 12-electrode and 16-electrode respectively. As a result, the response surfaces gave good estimations for FE data even for extrapolations delamination location/size for basalt FRP laminate composite pipe. On the other hand, it revealed that the estimation performance of delamination

location/size depends on the electrodes number, as the electrodes number increased the estimation performance is improved.
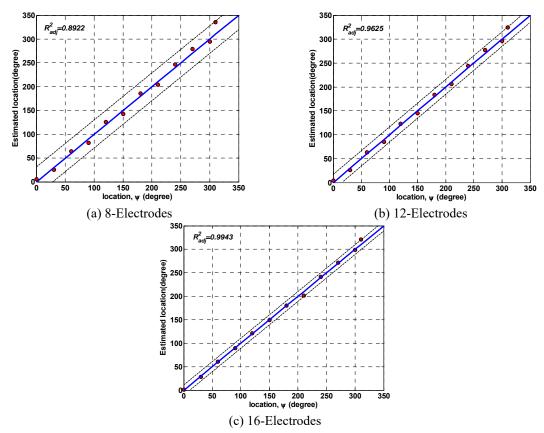

(a) 8-Electrodes   (b) 12-Electrodes

(c) 16-Electrodes

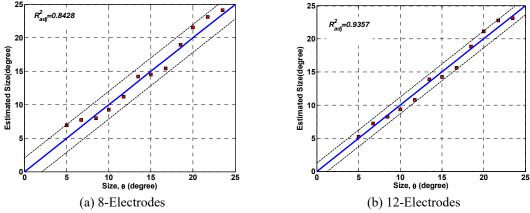Fig. 7 A comparison between estimation results of delamination Location, Ψ in basalt FRP laminate composite pipe

(a) 8-Electrodes   (b) 12-Electrodes

Fig. 8 A comparison between estimation results of delamination size, θ in basalt FRP laminate composite pipe
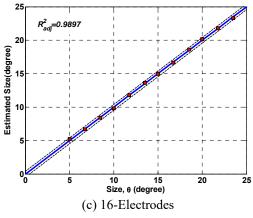
(c) 16-Electrodes

Fig. 8 Continued

6. Conclusions

The present study deals with the effect of the electrodes number for the electrical potential change (EPC) method to identify the delamination locations and size of basalt fiber reinforced polymer (FRP) laminated composite pipe. FE analyses are employed to investigate the effect here. The illustrated results are in excellent agreement with solutions available in the literature, thus validating the accuracy and reliability of the proposed technique. The response surfaces are used to solve the inverse problems. The results obtained are as follows:

1. The response surfaces that obtained from the FE data are provided excellent estimations of the delamination locations and size of basalt FRP pipe for each case of electrodes number, but a lot of FE calculations must be performed to obtain a sufficient number of data sets. This is the main drawback of the method identified so far.

2. The sensor sensitivity for delamination monitoring depends on the delamination size (θ) and the electrodes number are mounted on the outer surface of the basalt FRP pipe, as the electrodes number or delamination size (θ) increased, the sensor sensitivity is increased.

3. The estimation performance for delamination estimations increases with increasing the electrodes number are mounted on the outer surface of the basalt FRP pipe, with R^2_{adj} of location results are 0.8922, 0.9625 and 0.9943 for 8-electrode, 12-electrode and 16-electrode respectively and size results are 0.8428, 0.9357 and 0.9897 for 8-electrode, 12-electrode and 16-electrode respectively.

4. The error band for the delamination estimations depends on electrodes number mounted on the outer surface of the basalt FRP pipe, a larger number electrodes is required to maintain a high estimation performance for identifications.

References

Al-Tabey, W.A. (2010), "Effect of pipeline filling material on electrical capacitance tomography", *Proceedings of the International Postgraduate Conference on Engineering (IPCE 2010)*, Perlis, Malaysia, October.

Al-Tabey, W.A. (2012), *Finite Element Analysis in Mechanical Design Using ANSYS: Finite Element*

Analysis (FEA) Hand Book For Mechanical Engineers With ANSYS Tutorials, LAP Lambert Academic Publishing, Germany, ISBN 978-3-8454-0479-0.

Altabey, W.A. (2016), "Detecting and predicting the crude oil type inside composite pipes using ECS and ANN", *Struct. Monit. Mainten.*, **3**(4), 377-393.

Altabey, W.A. (2016), "FE and ANN model of ECS to simulate the pipelines suffer from internal corrosion", *Struct. Monit. Mainten.*, **3**(3), 297-314.

Altabey, W.A. (2016), "The thermal effect on electrical capacitance sensor for two-phase flow monitoring", *Struct. Monit. Mainten.*, **3**(4), 335-347.

Amaro, A.M., Santos, J.B. and Cirne, J.S. (2011), "Delamination depth in composites laminates with interface elements and ultrasound analysis", *Strain*, **47**(2), 138-145.

ANSYS Low-Frequency Electromagnetic analysis Guide, The Electrostatic Module in the Electromagnetic subsection of ANSYS, (2015), ANSYS, inc. Southpointe 275 Technology Drive Canonsburg, PA 15317, Published in the USA.

Asencio, K., Bramer-Escamilla, W., Gutiérrez, G. and Sánchez, I. (2015), "Electrical capacitance sensor array to measure density profiles of a vibrated granular bed", *J. Pow. Technol.*, **270**, 10-19.

Cunedioglu, Y. and Beylergil, B. (2015), "Free vibration analysis of damaged composite beams", *Struct. Eng. Mech.*, **55**(1), 79-92.

Daoye, Y., Bin, Z., Chuanlong, X., Guanghua, T. and Shimin, W. (2009), "Effect of pipeline thickness on electrical capacitance tomography", *Proceedings of the 6th International Symposium on Measurement Techniques for Multiphase Flows, Journal of Physics: Conference Series*, **147**, 1-13.

Davijani, A.A.B., Hajikhani, M. and Ahmadi, M. (2011), "Acoustic Emission based on sentry function to monitor the initiation of delamination in composite materials", *J. Mater. Des.*, **32**(5), 3059-3065.

De Albuquerque, V.C., Tavares, J.R.S. and Durão, L.M.P. (2010), "Evaluation of delamination damage on composite plates using an artificial neural network for the radiographic image analysis", *J. Compos. Mater.*, **44**(9), 1139-1159.

Fasching, G.E. and Smith, N.S. (1988), "High Resolution Capacitance Imaging System", US Dept. Energy, **37**, DOE/METC-88/4083.

Fasching, G.E. and Smith, N.S. (1991) "A capacitive system for 3-Dimensional imaging of fluidized-beds", *Rev. Sci. Instr.*, **62**(9), 2243-2251.

Garcia, D., Palazzetti, R., Trendafilova, I., Fiorini, C. and Zucchelli, A. (2015), "Vibration-based delamination diagnosis and modelling for composite laminate plates", *J. Compos. Struct.*, **130**, 155-162.

Heuer, H., Schulze, M.H. and Meyendorf, N. (2013), "Non-destructive evaluation (NDE) of composites: eddy current techniques", *Non-destructive evaluation (NDE) of polymer matrix composites: Techniques and applications*, 33-55.

Hu, N., Liu, Y., Li, Y., Peng, X. and Yan, B. (2010), "Optimal excitation frequency of lamb waves for delamination detection in CFRP laminates", *J. Compos. Mater.*, **44**(13), 1643-1663.

Huang, S.M., Plaskowski, A.B., Xie, C.G. and Beck, M.S. (1989), "Tomographic imaging of two-flow component flow using capacitance sensor", *J. Phys. E:Sci. Instrum.*, **22**, 173-177.

Jaworski, A.J. and Bolton, G.T. (2000), "The design of an electrical capacitance tomography sensor for use with media of high dielectric permittivity", *Measurement Sci. Technol.*, **11**(6), 743-757.

Jiang, S., Li, D., Zhou, C. and Zhang, L. (2014), "Capabilities of stochastic response surface method and response surface method in reliability analysis", *Struct. Eng. Mech.*, **49**(1), 111-128.

Li, H. and Huang, Z. (2000), "Special measurement technology and application", Zhejiang University Press, Hangzhou.

Liu, Z., Yu, H., He, C. and Wu, B. (2013), "Delamination damage detection of laminated composite beams using air-coupled ultrasonic transducers", *Sci. China Phys., Mech. Astronomy*, **56**(7), 1269-1279.

Liu, Z., Yu, H., He, C. and Wu, B. (2014), "Delamination detection in composite beams using pure Lamb mode generated by air-coupled ultrasonic transducer", *J. Intel. Mater. Syst. Struct.*, **25**(5), 541-550.

Mohamad, E.J., Rahim, R.A., Leow, P.L., Fazalul, Rahiman, M.H., Marwah, O.M.F., Nor Ayob, N.M., Rahim, H.A. and Mohd Yunus, F.R. (2012), "An introduction of two differential excitation potentials technique in electrical capacitance tomography", *J. Sens. Actuat. A*, **180**, 1-10.

Mohamad, E.J., Rahim, R.A., Rahiman, M.H.F., Ameran, H.L.M., Muji, S.Z.M. and Marwah, O.M.F. (2016), "Measurement and analysis of water/oil multiphase flow using Electrical Capacitance Tomography sensor", *J. Flow Measure. Instrument.*, **47**, 62-70.

Myers, R. and Montgomery, D.C. (2002), "Response surface methodology process and product optimization using designed experiments", 2nd ed. New York: Wiley-Interscience.

Nguyen, K., Ho, D. and Kim, J. (2013), "Damage detection in beam-type structures via PZT", *Smart Struct. Syst.*, **11**(2), 217-240.

Pei, T. and Wang, W. (2009), "Simulation analysis of sensitivity for electrical capacitance tomography", *Proceedings of Ninth International Conference on Electronic Measurement & Instruments (ICEMI 2009)*.

Peng, Q., Zhang, X., Huang, C., Carter, E.A. and Lu, G. (2012), "Hierarchical fiber-optic delamination detection system for carbon fiber reinforced plastic structures", *J. Model. Simulat. Mater. Sci. Eng.*, **18**, 1-14.

Saeedifar, M., Fotouhi, M., Najafabadi, M.A. and Toudeshky, H.H. (2015), "Prediction of delamination growth in laminated composites using acoustic emission and Cohesive Zone Modeling techniques", *J. Compos. Struct.*, **124**, 120-127.

Saeedifar, M., Fotouhi, M., Najafabadi, M.A., Toudeshky, H.H. and Minak, G. (2016), "Prediction of quasi-static delamination onset and growth in laminated composites by acoustic emission", *J. Compos. Part B: Eng.*, **85**, 113-122.

Sardeshpande, M.V., Harinarayan, S. and Ranade, V.V. (2015), "Void fraction measurement using electrical capacitance tomography and high speed photography", *J. Chem. Eng. Res. Des.*, **9**(4), 1-11.

Spiegel, M.D. (2014), "Damage detection in composite materials using PZT actuators and sensors for structural health monitoring", Master, Department of Electrical and Computer Engineering, University of Alabama.

Todoroki, A., Tanaka, Y. and Shimamura, Y. (2004), "Multi-prove electric potential change method for delamination monitoring of graphite/epoxy composite plates using normalized response surfaces", *J. Compos. Sci. Technol.*, **64**, 749-758.

Tompson, C.G. and Johnson, W.S. (2011), "Determination of the nontraditional lay-up influence and loading configuration on fatigue damage development under bearing-bypass loading conditions using radiography", *J. Compos. Mater.*, **45**(22), 2259-2269.

Toscano, C., Riccio, A., Camerlingo, F. and Meola, C. (2012), "Lock in thermography to monitor propagation of delamination in CFRP composites during compression tests", *11th International Conference on Quantitative InfraRed Thermography*, Naples, Italy, June.

Yang, W.Q. (1997), "Modelling of capacitance sensor", *IEEE proceedings: Measurement Science and Technology*, **144**(5), 203-208.

Yang, W.Q. and York, T.A. (1999), "New AC-based capacitance tomography system", *IEEE proceedings: Measurement Science and Technology*, **146**(1), 47-53.

Yang, W.Q., Beck, M.S. and Byars, M. (1995b), "Electrical capacitance tomography -from design to applications", *Measure. Control*, **28**(9), 261-266.

Yang, W.Q., Stott, A.L., Beck, M.S. and Xie, C.G. (1995a), "Development of capacitance tomographic imaging systems for oil pipeline measurements", *Rev. Sci. Instr.*, **66**(8), 4326.

Yeum, C.M., Sohn, H., Ihn, J.B. and Lim, H.J. (2012), "Delamination detection in a composite plate using a dual piezoelectric transducer network", *J. Compos. Struct.*, **94**, 3490-3499.

Zhang, W., Wang, C., Yang, W. and Wang, C. (2014), "Application of electrical capacitance tomography in particulate process measurement - A review", *J. Adv. Pow. Technol.*, **25**(1), 174-188.

TY